ChemComm

RSC Publishing

COMMUNICATION

View Article Online
View Journal | View Issue

# Fabrication of artificial toroid nanostructures by modified β-sheet peptides†

Cite this: *Chem. Commun.*, 2013, **49**, 8238

Received 5th June 2013,
Accepted 17th July 2013

DOI: 10.1039/c3cc44238a

www.rsc.org/chemcomm

Wen Li,* Jingfang Li and Myongsoo Lee*



**Facial peptide P1 carrying repeating hydrophobic and hydrophilic residues as well as lysine terminals self-assemble into uniform toroid structures. The sensitive balance between the hydrophobic interactions and electrostatic repulsion dominates the formation of highly curved assemblies.**

In recent years, artificial nanostructures based on peptide self-assembly have been of immense interest to the fields of nanotechnology, supramolecular chemistry and materials science.[1–3] This interest stems from the fact that these artificial nanostructures not only provide the possibility of developing biocompatible nanomaterials[4,5] but also allow mimicking the bio-nanostructures and/or the functional properties of biological origin, such as proteins and many subcellular organelles.[6] Toroid-like nanostructure is an important structural motif commonly found in many transmembrane proteins.[7] Water-soluble triosephosphate isomerase (TIM) β-barrel folds and the well-known green fluorescent protein family are typical toroid-like assemblies.[8] In general, these β-barrel folds adopt a closed structure in which the first and the last β-strands in a polypeptide chain are connected by hydrogen bonding. Inspired by the β-barrel proteins, pioneering studies have been performed on the development of artificial toroid nanostructures by introducing large hydrophilic side groups into β-sheet peptides.[9–11] These synthetic peptides show the capability to form unique annular shape with an internal pore in the central region in aqueous solution because the bulky effect of the large hydrophilic side groups causes the formation of interfacial curvatures. The efforts to fabricate a toroidal assembly also provide a novel approach to create artificial transmembrane channels.[11] Although the concept of interfacial curvatures provides a guiding principle to fabricate toroid peptides, examples of toroid assembly are still scarce due to the complicated procedures. In other words, the strategy of the bulky effect usually needs very complicated and multi-step chemical reactions in peptide synthesis. Therefore, the key challenge to fabricating toroid assemblies is how to develop a simple strategy through rational β-sheet peptide design to produce interfacial curvatures.

A lot of studies have shown that the self-assembly of the β-sheet peptides is determined by the synergistic driving forces behind the molecular self-assembly, including hydrophobic, electrostatic, hydrogen bonding and π–π interactions.[12,13] There is a general view on the self-assembly of β-sheet peptides: the strong hydrophobic and π–π interactions as well as directional hydrogen bonding between β-sheet peptide backbones facilitate one dimensional (1D) growth of nanostructure;[14,15] the electrostatic repulsion between hydrophilic heads could induce the formation of curvatures.[16] This situation led us to consider that it is possible to create discrete toroid nanostructures through simple weakening of the hydrophobic interactions and increasing the electrostatic repulsion of peptides. With this idea in mind, we designed a kind of facial peptide (**P1**) containing tryptophan units, tyrosine derivatives with tri(ethylene glycol) monomethyl ether, and terminal lysine units (Scheme 1). It is expected that the repeating hydrophilic and hydrophobic residues could promote the formation of a β-sheet conformation with suitable strength, and the protonated lysine heads in aqueous solution could provide electrostatic repulsion to create curvatures. Herein, we present the toroidal self-assembly of the peptide **P1**. To elucidate the delicate balance between electrostatic repulsions

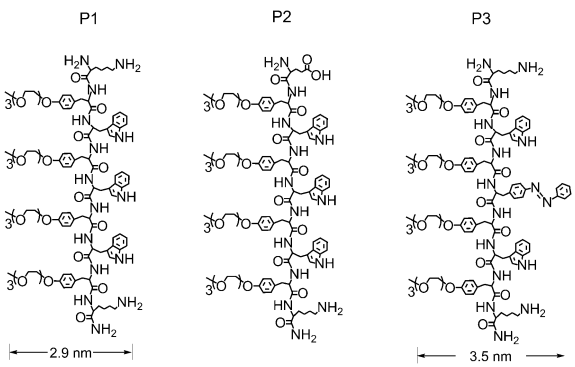


**Scheme 1** Molecular structures of the synthesized peptides **P1**, **P2** and **P3**.

*State Key Laboratory of Supramolecular Structure and Materials, College of Chemistry, Jilin University, Changchun 130012, China. E-mail: wenli@jlu.edu.cn, mslee@jlu.edu.cn; Fax: +86-0431-85193421; Tel: +86-0431-85168499*

† Electronic supplementary information (ESI) available: Experimental details of peptide synthesis and characterization, CD and DLS spectra, and additional TEM images. See DOI: 10.1039/c3cc44238a

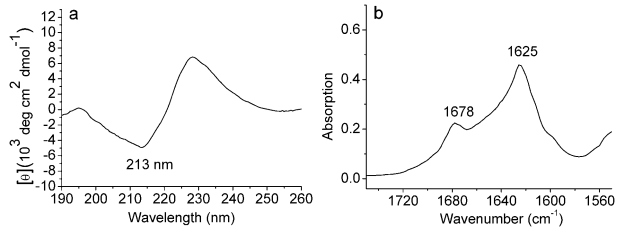


**Fig. 1** (a) Circular dichroism (CD) spectrum of **P1** aqueous solution (pH ~ 6.7); (b) FT-IR spectrum of **P1**.

and the hydrophobic interactions, two analogous peptides **P2** and **P3** were synthesized. All these peptides were synthesized employing a standard Fmoc solid-phase method. The successful synthesis and the purification have been confirmed by MALDI-TOF-MS spectrometry and HPLC (Fig. S1 and S2, see ESI†).

The circular dichroism (CD) spectrum of **P1** aqueous solution displayed a negative Cotton effect at 213 nm (Fig. 1a), indicating the β-strand conformation. The Fourier transform infrared (FT-IR) spectrum of **P1** showed well-defined amide I bands centred at 1625 $cm^{-1}$ and 1678 $cm^{-1}$ (Fig. 1b), suggesting an antiparallel β-strand arrangement.[17,18] Dynamic light scattering (DLS) showed the presence of assemblies in solution, mostly with 18 nm in diameter (Fig. S3†).

When **P1** aqueous solution (40 μM, pH ≅ 6.7) was cast onto a copper grid and thereafter negatively stained with uranyl acetate, highly curved toroid structures were observed from the transmission electron microscopy (TEM). As shown in Fig. 2a, the diameter of the toroid exterior and the internal pore was measured to be 10.5 ± 0.2 nm and 3.5 ± 0.2 nm, respectively. The size of the toroid structures calculated from the TEM image is smaller than that obtained from DLS, which probably arises from the solvent evaporation accompanied by the shrinkage of the assemblies. The cryogenic TEM (cryoTEM) image obtained from the 40 μM aqueous solution of **P1** confirmed the formation of toroid structures (Fig. 2b). The electron density at the central part is clearly lower than that at the edge of the assemblies, indicating the presence of hollow structures.

The wall thickness of the toroid assemblies is about 3.1 ± 0.2 nm (Fig. 2a, inset), which is consistent with the molecular length of 2.9 nm. The result indicates that the toroids are composed of a single layer of the **P1** molecules in which the backbones of β-sheet peptides are oriented perpendicularly to the plane of the rings. Considering the amphiphilic feature of **P1**, the hydrophilic face should be exposed to water, while the hydrophobic face (tryptophan residues) is located inside the toroid assemblies to reduce its contact with water, as shown in Fig. 2c. We presumed that the formation of discrete toroid structures with highly interfacial curvatures originated from the electrostatic repulsions of protonated lysine groups because of their high p$K_a$ value (p$K_a$ ~ 10). To prove this speculation, we studied the self-assembly behavior of **P1** after treatment with salts (sodium chloride) and alkaline reagents (ammonia water). In these cases, the electrostatic repulsions between lysine groups would be suppressed significantly. **P1** formed long nanoribbons when the pH value of aqueous solution was above 10 (Fig. 3a) or the salt concentration was over 200 mM (Fig. S4, ESI†). Notably, these peptide nanoribbons obtained from alkaline aqueous solution can reversibly transform into toroid nanostructures after acidifying the solution to pH ≅ 7 (Fig. 3b).

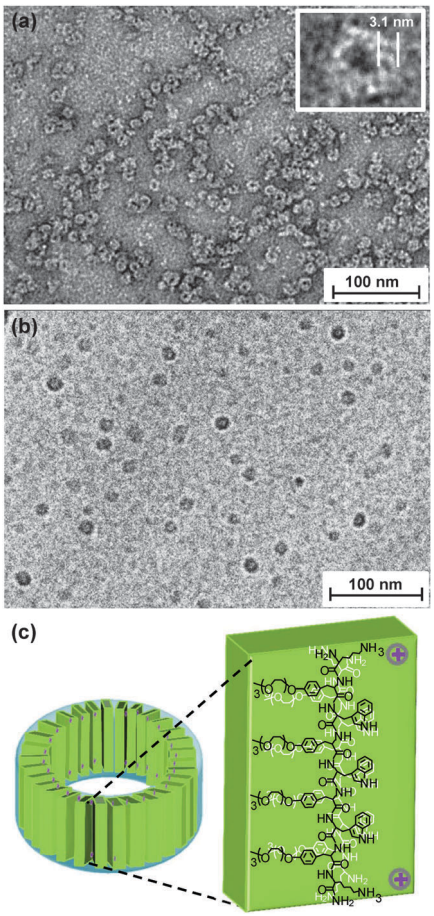


**Fig. 2** TEM (a), cryo-TEM (b) and the self-assembly model (c) of peptide **P1** obtained from 40 μM aqueous solution (pH ~ 6.7) (a, inset: high-magnification TEM image of a single toroid).

To scrutinize the electrostatic repulsion, we also prepared the analogous one bearing a glutamic acid at one end of the peptide molecule (Scheme 1, **P2**). As expected, peptide **P2** self-assembled into long nanoribbons (Fig. S5, ESI†) based on electrostatic interactions between glutamic acid and lysine units of the adjacent molecules.

The above results strongly demonstrate that the electrostatic repulsions of protonated lysine groups between adjacent **P1** molecules not only can reduce the strength of β-sheets and inhibit the 1D growth, but also can induce high interfacial curvatures, leading to the formation of discrete toroids. The removal of the electrostatic repulsions reduced the interfacial curvature and increased the interactions of **P1** as well. Eventually, the enhanced β-sheet strength of peptide molecules caused the formation of 1D nanoribbons.

To gain further insight into the β-sheet strength of peptide **P1**, we have prepared the analogous one through replacing the middle indole side group of **P1** by a comparatively hydrophobic azobenzene segment in peptide **P3** (Scheme 1). This molecular design would enhance the β-sheet strength through increased hydrophobic interactions between adjacent peptide molecules, and retain the electrostatic repulsions as well. In significant contrast to **P1**, the TEM image of **P3** showed helical ribbons together with some bundled double helices (Fig. 4 and inset). The helical structure has a cross-sectional width ($d$) of 5.3 ± 0.3 nm, and persistence lengths on the order of several hundred nanometers.

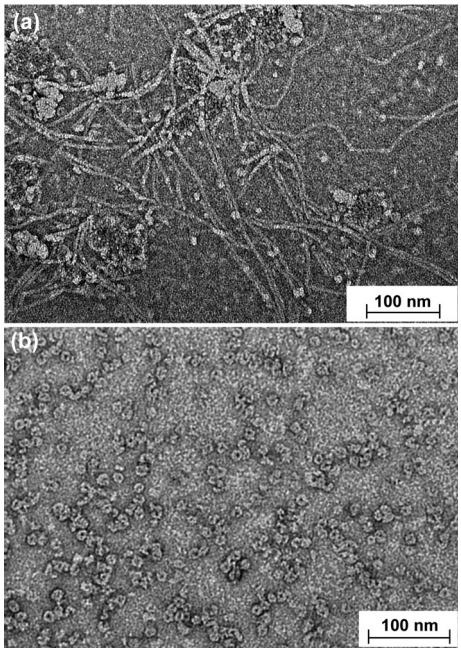


**Fig. 3** (a) TEM image of **P1** obtained from 40 μM alkaline aqueous solution (pH ~ 10.5); (b) TEM image of **P1** after acidifying the alkaline solution to pH ~ 7.

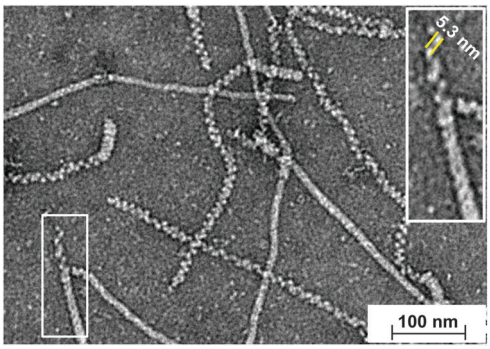


**Fig. 4** TEM image of peptide **P3** obtained from 40 μM aqueous solution (inset: high-magnification TEM image of a bundled double helix).

The appearance of the helical structure in aqueous solution was also confirmed by cryo-TEM (Fig. S6, ESI†). Analysis of several TEM images of the helical ribbons shows that the assemblies have both left-handed and right-handed periodicities (Fig. S7, ESI†). The above observation indicates that increasing the hydrophobic interactions enforced the peptide molecules to associate with each other to form extended 1D nanostructures. Again, the highly curved helices originate from the electrostatic repulsions between the protonated lysine heads of **P3** because the twisted β-sheet arrangement allows the minimization of the electrostatic repulsions of adjacent molecules.[19] We thus propose that the toroid assemblies of **P1** arise from the delicate balance between hydrophobic interactions and the electrostatic repulsions.

In summary, we have described the self-assembly of very short peptides consisting of alternating hydrophobic and hydrophilic segments, and lysine ends as well. Peptide **P1** self-assembled into highly uniform and discrete toroid morphology. However, removing the electrostatic repulsions or increasing the hydrophobic interactions of peptides drove the β-sheet peptides to form extended 1D nanostructures. It is proposed that the delicate synergy among the hydrophobic interactions and the opposing charge repulsion are very important in terms of the factors dominating the toroid assemblies. Ultimately, this study has described a facile strategy to fabricate toroid nanostructures through weakening the hydrophobic interactions and increasing the electrostatic repulsion by the rationally designed peptide building blocks.

This work was supported by the National Natural Science Foundation of China (50973042, 21221063) and the 111 project (B06009). We thank Seong-Kyun Kang and Il-soo Park for assistance with the TEM experiment at Seoul National University.

## Notes and references

1 H. A. Lashuel, D. Hartley, B. M. Petre, T. Walz and P. T. Lansbury, *Nature*, 2002, **418**, 291–292.
2 E. Cohen, J. Bieschke, R. M. Perciavalle, J. W. Kelly and A. Dillin, *Science*, 2006, **313**, 1604–1610.
3 (*a*) I. Cherny and E. Gazit, *Angew. Chem., Int. Ed.*, 2008, **47**, 4062–4069; (*b*) M.-T. Popescu, S. Mourtas, G. Pampalakis, S. G. Antimisiaris and C. Tsitsilianis, *Biomacromolecules*, 2011, **12**, 3023–3030; (*c*) Y. Zhang, Y. Kuang, Y. Gao and B. Xu, *Langmuir*, 2011, **27**, 529–537; (*d*) S. Kyle, A. Aggeli, E. Ingham and M. J. McPherson, *Biomaterials*, 2010, **31**, 9395–9405.
4 (*a*) X. Li, Y. Kuang, J. Shi, Y. Gao, H.-C. Lin and B. Xu, *J. Am. Chem. Soc.*, 2011, **133**, 17513–17518; (*b*) X. B. Zhao, F. Pan, H. Xu, M. Yaseen, H. H. Shan, C. A. E. Hauser, S. G. Zhang and J. R. Lu, *Chem. Soc. Rev.*, 2010, **39**, 3480–3498.
5 M. J. Webber, J. Tongers, C. J. Newcomb, K.-T. Marquardt, J. Bauersachs, D. W. Losordo and S. I. Stupp, *Proc. Natl. Acad. Sci. U. S. A.*, 2011, **108**, 13438–13443.
6 (*a*) L. F. Fraceto, J. S. Oyama, C. R. Nakaie, A. Spisni, E. de Paula and T. A. Pertinhez, *Biophys. Chem.*, 2006, **123**, 29–39; (*b*) A. M. Tamburro, A. Pepe and B. Bochicchio, *Biochemistry*, 2006, **45**, 9518–9530.
7 W. C. Wimley, *Curr. Opin. Struct. Biol.*, 2003, **13**, 404–411.
8 R. K. Wierenga, *FEBS Lett.*, 2001, **492**, 193–198.
9 Y.-B. Lim, E. Lee and M. Lee, *Macromol. Rapid Commun.*, 2011, **32**, 191–196.
10 Y.-B. Lim, K.-S. Moon and M. Lee, *Angew. Chem., Int. Ed.*, 2009, **48**, 1601–1605.
11 I.-S. Park, Y.-R. Yoon, M. Jung, K. Kim, S. B. Park, S. Shin, Y.-B. Lim and M. Lee, *Chem.–Asian. J.*, 2011, **6**, 452–458.
12 (*a*) E. Gazit, *Chem. Soc. Rev.*, 2007, **36**, 1263–1269; (*b*) J. Kopecek and J. Yang, *Angew. Chem., Int. Ed.*, 2012, **51**, 7396–7417.
13 (*a*) C. Tomasini and N. Castellucci, *Chem. Soc. Rev.*, 2013, **42**, 156–172; (*b*) R. Ni, W. S. Childers, K. I. Hardcastle, A. K. Mehta and D. G. Lynn, *Angew. Chem., Int. Ed.*, 2012, **51**, 6635–6638.
14 (*a*) S. E. Paramonov, H. W. Jun and J. D. Hartgerink, *J. Am. Chem. Soc.*, 2006, **128**, 7291–7298; (*b*) S. Marchesan, Y. Qu, L. J. Waddington, C. D. Easton, V. Glattauer, T. J. Lithgow, K. M. McLean, J. S. Forsythe and P. G. Hartley, *Biomaterials*, 2013, **34**, 3678–3687; (*c*) E. T. Pashuck, H. Cui and S. I. Stupp, *J. Am. Chem. Soc.*, 2010, **132**, 6041–6046.
15 (*a*) H. Z. Huang, J. Shi, J. Laskin, Z. Liu, D. S. McVey and X. S. Sun, *Soft Matter*, 2011, **7**, 8905–8912; (*b*) C. Ou, J. Zhang, X. Zhang, Z. Yang and M. Chen, *Chem. Commun.*, 2013, **49**, 1853–1855.
16 (*a*) M. N. Bongiovanni, F. Caruso and S. L. Gras, *Soft Matter*, 2013, **9**, 3315–3330; (*b*) S. Han, S. Cao, Y. Wang, J. Wang, D. Xia, H. Xu, X. Zhao and J. R. Lu, *Chem.–Eur. J.*, 2011, **17**, 13095–13102.
17 P. Kupser, K. Pagel, J. Oomens, N. C. Polfer, B. Koksch, G. Meijer and G. von Helden, *J. Am. Chem. Soc.*, 2010, **132**, 2085–2093.
18 (*a*) H. Ceylan, M. Urel, T. S. Erkal, A. B. Tekinay, A. Dana and M. O. Guler, *Adv. Funct. Mater.*, 2013, **23**, 2081–2090; (*b*) S. Marchesan, L. Waddington, C. D. Easton, D. A. Winkler, L. Goodall, J. Forsythe and P. G. Hartley, *Nanoscale*, 2012, **4**, 6752–6760.
19 C. J. Bowerman, W. Liyanage, A. J. Federation and B. L. Nilsson, *Biomacromolecules*, 2011, **12**, 2735–2745.

 